PROCEEDINGS OF SCIENCE

Simultaneous QCD analysis for identified and unidentified light charged hadrons

M. Soleymaninia,[a,*] **M. Goharipour,**[a] **H. Khanpou**[b] **and H. Spiesberger**[c]

[a] *School of Particles and Accelerators, Institute for Research in Fundamental Sciences (IPM), P.O.Box 19395-5531, Tehran, Iran*

[b] *Department of Physics, University of Science and Technology of Mazandaran, P.O.Box 48518-78195, Behshahr, Iran*

[c] *PRISMA$^+$ Cluster of Excellence, Institut für Physik, Johannes-Gutenberg-Universität, Staudinger Weg 7, D-55099 Mainz, Germany*

E-mail: Maryam_Soleymaninia@ipm.ir, Muhammad.Goharipour@ipm.ir, HKhanpour@mazust.ac.ir, spiesber@uni-mainz.de

In this paper, we determine the precise fragmentation functions (FFs) of charged pions ($\pi^{\pm}$), charged kaons ($K^{\pm}$), proton/antiprotons ($p/\bar{p}$) as well as unidentified light charged hadrons ($h^{\pm}$). This determination is performed through a simultaneous QCD analysis of all available experimental data from single-inclusive hadron production in electron-positron annihilation (SIA) processes for $\pi^{\pm}, K^{\pm}, p/\bar{p}$ and $h^{\pm}$ production. Our results show that these data have significant impact on both size and uncertainties of the FFs. We apply higher-order perturbative QCD corrections up to next-to-next-to-leading order (NNLO) and also include finite-hadron mass effects.

**** The European Physical Society Conference on High Energy Physics (EPS-HEP2021), ****
**** 26-30 July 2021 ****
**** Online conference, jointly organized by Universität Hamburg and the research center DESY ****

[*] Speaker

PoS(EPS-HEP2021)407

1. Introduction

There have been several QCD analyses to extract the fragmentation functions (FFs) of pions, kaons, protons, and unidentified light charged hadrons individually [1–8], in which experimental data from different processes have been used, such as single inclusive hadron production in electron-positron annihilation (SIA), semi-inclusive deep inelastic scattering (SIDIS), and from proton-(anti)proton collisions. However, they are different in other aspects, such as the phenomenological framework, the QCD perturbative order and the error calculation procedure. The main goal of the present study is to develop our previous analysis [9] to calculate the FFs for charged pions ($\pi^{\pm}$), charged kaons ($K^{\pm}$), proton/antiproton ($P/\bar{(P)}$) and unidentified light charged hadrons ($h^{\pm}$) simultaneously by using all SIA data for these hadrons production. Our results show this simultaneous QCD analysis along with considering hadron mass corrections up to next-to-next-to-leading order (NNLO) accuracy, improves the fit quality significantly and leads to well-constrained FFs.

2. The QCD framework

Unidentified light charged hadrons include $\pi^{\pm}, K^{\pm}, p/\bar{p}$, and residual light charged hadrons whose contributions are small in comparison with pion, kaon and proton. Hence, the FFs of unidentified light charged hadrons are given by

$$D_i^{h^{\pm}} = D_i^{\pi^{\pm}} + D_i^{K^{\pm}} + D_i^{p/\bar{p}} + D_i^{res^{\pm}} . \tag{1}$$

We parametrize the pion, kaon and proton FFs at the initial scale $Q_0 = 5$ GeV by the following functional form [10]:

$$D_i^{\pi^{\pm},K^{\pm},p/\bar{p}}(z,Q_0) = \frac{\mathcal{N}_i z^{\alpha_i}(1-z)^{\beta_i}[1+\gamma_i(1-z)^{\delta_i}]}{B[2+\alpha_i,\beta_i+1]+\gamma_i B[2+\alpha_i,\beta_i+\delta_i+1]}, \tag{2}$$

where $i = u^+, d^+, s^+, c^+, b^+$ and gluon g, with $q^+ = q+\bar{q}$. For pion FFs, we assume isospin symmetry $D_{u^+}^{\pi^{\pm}} = D_{d^+}^{\pi^{\pm}}$. However for kaon, we allow all light flavor FFs to be different $D_{u^+}^{K^{\pm}} \neq D_{d^+}^{K^{\pm}} \neq D_{s^+}^{K^{\pm}}$. We consider a relation between u^+ and d^+ FFs for proton by a z independent normalization factor $D_{u^+}^{p/\bar{p}} = \mathcal{N} D_{d^+}^{p/\bar{p}}$.

The residual light hadrons contribution is rather small, and we consider a simple parametrization function for the residual light charged hadrons FFs given by

$$D_i^{\text{res}^{\pm}}(z,Q_0) = \mathcal{N}_i \frac{z^{\alpha_i}(1-z)^{\beta_i}}{B[2+\alpha_i,\beta_i+1]}, \tag{3}$$

where i refers to d^+, u^+, s^+, c^+, b^+, and g. The $SU(3)$ flavor symmetry of light quark flavors is applied for residual hadron FFs, $D_{u^+}^{\text{res}^{\pm}} = D_{d^+}^{\text{res}^{\pm}} = D_{s^+}^{\text{res}^{\pm}}$.

3. Results and discussions

In this section, we systematically study our analysis and the additional constraints due to the inclusion of unidentified charged hadron experimental data. For this purpose, we first determine

the pion, kaon, and proton FFs by performing three separate analyses of the related SIA data as usual. Then we include also the unidentified light charged hadron measurements and perform a simultaneous analysis of all data to study how it affects the extracted FFs. The results obtained for the $\pi^{\pm}, K^{\pm}$ and $p/\bar{p}$ FFs from these two approaches at the scale $Q^2 = 100$ GeV^2 are compared in Figs. 1, 2 and 3, respectively, where all FFs have been normalized to their central values calculated in the separate hadron fits.

As can clearly be seen from Figs. 1, 2 and 3, the inclusion of unidentified light hadron data modifies the central values and the uncertainties of FFs. In the case of the charged pion FF in Fig. 1, the reduction of the uncertainty bands is noticeable, especially for $D_g^{\pi^{\pm}}$ and $D_{\Sigma}^{\pi^{\pm}}$. Also, one can see the effect of including the unidentified light charged hadron data on the shape of gluon FF of pion. In Fig. 2, similarly, we can see the reduction of the uncertainties for $D_g^{K^{\pm}}$ and $D_{\Sigma}^{K^{\pm}}$, but by a smaller factor in comparison to pion FFs. In the final case in Fig. 3 remarkable changes of the shapes can be seen for gluon and heavy quark FFs. Here again, a large decrease in the uncertainty bands is visible for all FFs except for the Σ FF.

We present here, in the last four columns of Table 1, the values of χ^2 per number of data points, $\chi^2/(N_{\text{pts.}})$, for each data set individually. The value of the total χ^2 per number of degrees of freedom, $\chi^2/(\text{d.o.f.})$, is shown in the last row of this table. It should be noted that the final number of data points of each experimental data set shown in the tables is subject to kinematic cuts. After imposing the kinematical cuts, our total number of data is $N_{\text{pts.}} = 1492$. In addition, we find $\chi^2/\text{d.o.f.} = 1.171$ for NLO and $\chi^2/\text{d.o.f.} = 1.083$ for NNLO fits and so the NNLO fit shows in general a better fit quality.

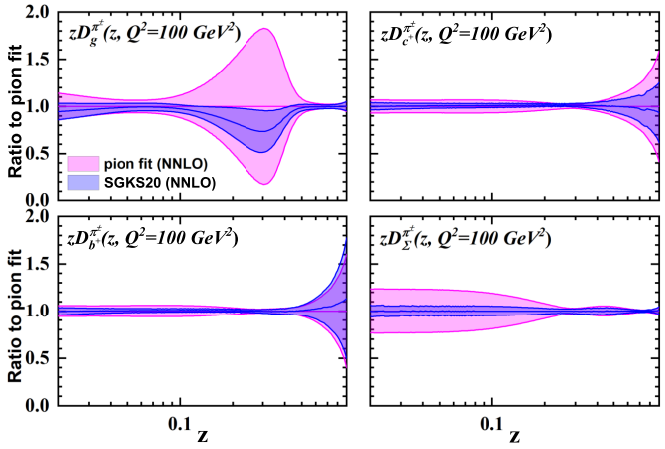

Figure 1: Comparison of SGKS20 NNLO charged pion FFs, $zD_i^{\pi^{\pm}}(z, Q^2 = 100\ \text{GeV}^2)$ $(i = g, c, b, \Sigma)$ obtained from a simultaneous analysis of all $\pi^{\pm}, K^{\pm}, p/\bar{p}$ and $h^{\pm}$ data with corresponding ones obtained from the analysis of $\pi^{\pm}$ data separately.

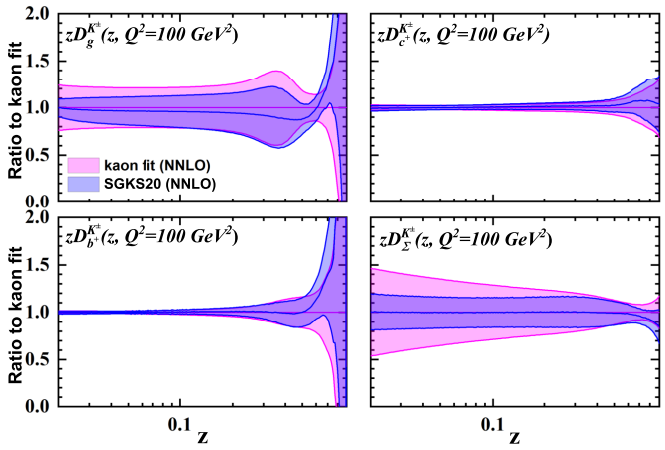

Figure 2: Same as Fig. 1, but for the charged kaon $zD_i^{K^\pm}(z, Q^2)$ FFs.

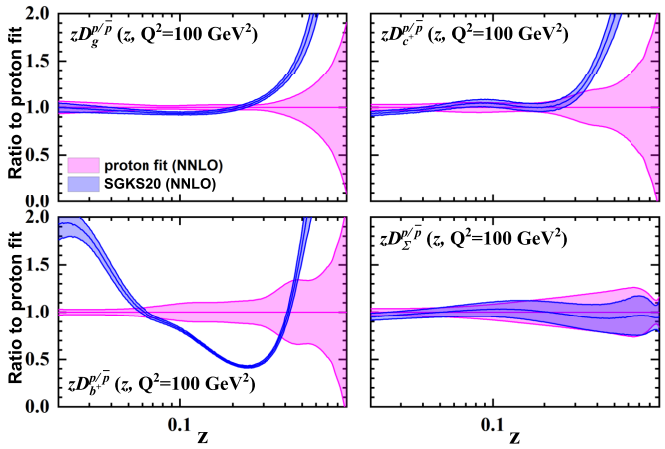

Figure 3: Same as Fig. 1, but for the proton and antiproton FFs, $zD_i^{p/\bar{p}}(z, Q^2)$.

References

[1] R. A. Khalek, V. Bertone and E. R. Nocera, Phys. Rev. D **104** (2021) no.3, 034007 doi:10.1103/PhysRevD.104.034007 [arXiv:2105.08725 [hep-ph]].

[2] E. Moffat *et al.* [Jefferson Lab Angular Momentum (JAM)], Phys. Rev. D **104**, no.1, 016015 (2021) doi:10.1103/PhysRevD.104.016015 [arXiv:2101.04664 [hep-ph]].

[3] V. Bertone *et al.* [NNPDF Collaboration], Eur. Phys. J. C **78**, 651 (2018), [arXiv:1807.03310 [hep-ph]].

[4] M. Soleymaninia, M. Goharipour and H. Khanpour, Phys. Rev. D **98**, 074002 (2018), [arXiv:1805.04847 [hep-ph]].

[5] V. Bertone *et al.* [NNPDF Collaboration], Eur. Phys. J. C **77**, 516 (2017), [arXiv:1706.07049 [hep-ph]].

[6] M. Epele, C. García Canal and R. Sassot, Phys. Lett. B **790**, 102 (2019), [arXiv:1807.07495 [hep-ph]].

[7] D. de Florian, R. Sassot, M. Epele, R. J. Hernández-Pinto and M. Stratmann, Phys. Rev. D **91**, 014035 (2015), [arXiv:1410.6027 [hep-ph]].

[8] D. de Florian, M. Epele, R. J. Hernández-Pinto, R. Sassot and M. Stratmann, Phys. Rev. D **95**, 094019 (2017), [arXiv:1702.06353 [hep-ph]].

[9] M. Soleymaninia, M. Goharipour and H. Khanpour, Phys. Rev. D **99**, 034024 (2019), [arXiv:1901.01120 [hep-ph]].

[10] M. Soleymaninia, M. Goharipour, H. Khanpour and H. Spiesberger, Phys. Rev. D **103**, no.5, 054045 (2021) doi:10.1103/PhysRevD.103.054045 [arXiv:2008.05342 [hep-ph]].

[11] M. Leitgab *et al.* [Belle Collaboration], Phys. Rev. Lett. **111**, 062002 (2013), [arXiv:1301.6183 [hep-ex]].

[12] J. P. Lees *et al.* [BaBar Collaboration], Phys. Rev. D **88**, 032011 (2013), [arXiv:1306.2895 [hep-ex]].

[13] R. Brandelik *et al.* [TASSO Collaboration], Phys. Lett. **94B**, 444 (1980).

[14] W. Braunschweig *et al.* [TASSO Collaboration], Z. Phys. C **47**, 187 (1990).

[15] H. Aihara *et al.* [TPC/Two Gamma Collaboration], Phys. Rev. Lett. **61**, 1263 (1988).

[16] W. Braunschweig *et al.* [TASSO Collaboration], 5"Pion, Kaon and Proton Cross-sections in e^+e^- Z. Phys. C **42**, 189 (1989).

[17] D. Buskulic *et al.* [ALEPH Collaboration], Z. Phys. C **66**, 355 (1995).

[18] D. Buskulic *et al.* [ALEPH Collaboration], Phys. Lett. B **357**, 487 (1995), Erratum: [Phys. Lett. B **364**, 247 (1995)].

[19] P. Abreu *et al.* [DELPHI Collaboration], Eur. Phys. J. C **5**, 585 (1998).

[20] R. Akers *et al.* [OPAL Collaboration], Z. Phys. C **63**, 181 (1994).

[21] K. Ackerstaff *et al.* [OPAL Collaboration], Eur. Phys. J. C **7**, 369 (1999), [hep-ex/9807004].

[22] K. Abe *et al.* [SLD Collaboration], Phys. Rev. D **69**, 072003 (2004), [hep-ex/0310017].

[23] M. Althoff *et al.* [TASSO Collaboration], Z. Phys. C **17**, 5 (1983).

Experiment	$\sqrt{s}$	$\frac{\chi^2}{N_{\text{pts.}}}(\pi^{\pm})$	$\frac{\chi^2}{N_{\text{pts.}}}(K^{\pm})$	$\frac{\chi^2}{N_{\text{pts.}}}(p/\bar{p})$	$\frac{\chi^2}{N_{\text{pts.}}}(h^{\pm})$
BELLE [11]	10.52	0.295	0.993	—	—
BABAR [12]	10.54	1.504	2.503	0.234	—
TASSO12 [13]	12	1.135	0.933	0.669	—
TASSO14 [14, 23]	14	1.194	1.392	2.166	0.627
TASSO22 [14, 23]	22	2.348	2.580	1.920	0.697
TPC [15]	29	1.099	0.519	4.814	0.438
TASSO30 [13]	30	—	—	1.339	—
TASSO34 [16]	34	1.136	0.175	1.496	—
TASSO35 [14]	34	—	—	—	1.362
TASSO44 [14, 16]	44	2.129	—	—	0.799
ALEPH [17, 18]	91.2	1.362	0.747	0.991	0.738
DELPHI (incl.) [19]	91.2	1.471	0.684	0.541	0.508
DELPHI (uds tag) [19]	91.2	0.991	1.050	0.578	0.413
DELPHI (b tag) [19]	91.2	0.850	0.651	1.537	0.295
OPAL (incl.) [20, 21]	91.2	1.380	1.126	—	0.780
OPAL (uds tag) [20, 21]	91.2	—	—	—	0.552
OPAL (c tag) [20, 21]	91.2	—	—	—	0.624
OPAL (b tag) [20, 21]	91.2	—	—	—	0.175
SLD (incl.) [22]	91.2	1.181	0.549	0.831	0.289
SLD (uds tag) [22]	91.2	1.186	2.065	1.197	0.604
SLD (c tag) [22]	91.2	0.818	0.992	3.661	0.617
SLD (b tag) [22]	91.2	0.667	1.282	2.664	0.140
Total χ^2/d.o.f.			1558.169/1438 = 1.083		

Table 1: The list of data sets for $\pi^{\pm}$, $K^{\pm}$, $p/\bar{p}$, and $h^{\pm}$ production used in the present analysis. For each input data set, we have indicated the corresponding reference and the center-of-mass energy. In the last four columns the value of $\chi^2/N_{\text{pts.}}$ resulting from the FF fit are shown at NNLO order. We show the total value of χ^2/d.o.f. at the bottom of the table.